Fibrosis in Human Adipose Tissue: Composition, Distribution, and Link With Lipid Metabolism and Fat Mass Loss

Adeline Divoux,[1] Joan Tordjman,[1] Danièle Lacasa,[2] Nicolas Veyrie,[1,3] Danielle Hugol,[1,4] Abdelhalim Aissat,[1,3] Arnaud Basdevant,[1,2] Michèle Guerre-Millo,[1] Christine Poitou,[1,2] Jean-Daniel Zucker,[1] Pierre Bedossa,[1,5] and Karine Clément[1,2]

OBJECTIVE—Fibrosis is a newly appreciated hallmark of the pathological alteration of human white adipose tissue (WAT). We investigated the composition of subcutaneous (scWAT) and omental WAT (oWAT) fibrosis in obesity and its relationship with metabolic alterations and surgery-induced weight loss.

RESEARCH DESIGN AND METHODS—Surgical biopsies for scWAT and oWAT were obtained in 65 obese (BMI 48.2 ± 0.8 kg/m^2) and 9 lean subjects (BMI 22.8 ± 0.7 kg/m^2). Obese subjects who were candidates for bariatric surgery were clinically characterized before, 3, 6, and 12 months after surgery, including fat mass evaluation by dual energy X-ray absorptiometry. WAT fibrosis was quantified and characterized using quantitative PCR, microscopic observation, and immunohistochemistry.

RESULTS—Fibrosis amount, distribution and collagen types (I, III, and VI) present distinct characteristics in lean and obese subjects and with WAT depots localization (subcutaneous or omental). Obese subjects had more total fibrosis in oWAT and had more pericellular fibrosis around adipocytes than lean subjects in both depots. Macrophages and mastocytes were highly represented in fibrotic bundles in oWAT, whereas scWAT was more frequently characterized by hypocellular fibrosis. The oWAT fibrosis negatively correlated with omental adipocyte diameters ($R = -0.30$, $P = 0.02$), and with triglyceride levels ($R = -0.42$, $P < 0.01$), and positively with apoA1 ($R = 0.25$, $P = 0.05$). Importantly, scWAT fibrosis correlated negatively with fat mass loss measured at the three time points after surgery.

CONCLUSIONS—Our data suggest differential clinical consequences of fibrosis in human WAT. In oWAT, fibrosis could contribute to limit adipocyte hypertrophy and is associated with a better lipid profile, whereas scWAT fibrosis may hamper fat mass loss induced by surgery. ***Diabetes*** **59:2817–2825, 2010**

From the [1]INSERM, U872, Nutriomique, Paris, France; Université Pierre et Marie Curie-Paris6, Centre de Recherche des Cordeliers, Paris, France; Université Paris Descartes, Paris, France; the [2]Assistance Publique-Hôpitaux de Paris, Nutrition and Endocrinology Department, Pitié-Salpêtrière Hospital, Paris, France; CRNH-Ile de France, Paris, France; the [3]Assistance Publique-Hôpitaux de Paris, Surgery Department, Hôtel-Dieu Hospital, Paris, France; the [4]Assistance Publique-Hôpitaux de Paris, Anatomopathology Department, Hôtel-Dieu Hospital, Paris, France; and the [5]Assistance Publique-Hôpitaux de Paris, Beaujon Hospital, Pathology Department, Clichy, France, and Centre de Recherche Bichat-Beaujon, INSERM U773, Clichy, France.

Corresponding authors: Karine Clément, karine.clement@psl.aphp.fr, and Joan Tordjman, joan.tordjman@crc.jussieu.fr.

Received 26 April 2010 and accepted 30 July 2010. Published ahead of print at http://diabetes.diabetesjournals.org on 16 August 2010. DOI: 10.2337/db10-0585.

A.D. and J.T. equally contributed to this study.

White adipose tissue (WAT) is the main energy repository in the body. It stores and mobilizes, according to body demand, fatty acids that have been implicated in the development of insulin resistance. In turns, the phenotype and the biology of WAT cellular components are altered by two major processes: adipose cell hypertrophy and immune cells accumulation. Inflammation, reticulum endoplasmic stress, and hypoxia are part of the biologic alterations that attract and retain inflammatory cells in WAT (1). Both adipocytes and nonadipose cells of the stromal vascular fraction of WAT have been implicated in the secretion of inflammatory molecules and in the development of insulin resistance (2,3). WAT extracellular matrix (ECM) remodeling, which plays a pivotal role in adipogenesis (4) and tissue architecture (5), is crucial to accommodate obesity-induced cellular alterations (6). However, the persistence of an inflammation stimulus in WAT may be responsible for an excessive synthesis of ECM components and subsequent interstitial deposition of fibrotic material. Fibrosis, attributed to excessive deposition of ECM proteins, is a ubiquitous tissue response to an unresolved chronic inflammation (7). We recently highlighted this phenomenon in obese WAT (8), showing increased expression of genes encoding extracellular matrix components and demonstrating the presence of fibrosis (8,9). In a small number of subjects, we scored histologic WAT fibrous tissue using a picrosirius red staining and observed an increased abundance of ECM in obese versus lean WAT (8). Moreover, we demonstrated that human adipocyte precursors secrete ECM components when challenged by macrophage secretions (10), emphasizing the prominence of macrophage-preadipocyte interactions in WAT fibrosis development or maintenance. Other inflammatory cells accumulate in obese WAT, including T-lymphocytes and mast cells (11), and might also participate in the orchestration of fibrosis deposition.

The nature and consequences of ECM modification in WAT have been investigated in mice. In *db/db* obese mice, various types of collagens are overexpressed in epididymal WAT (12). The predominantly expressed collagen mRNAs in epididymal WAT encode types I, IV, and VI. In mice deleted for the *col6a1* gene, the lack of collagen VI associates with increased adipocyte size, both in response to a high-fat diet and on the obese *ob/ob* genetic background (11). A similar phenotype of adipose cell hypertrophy has been reported in mice deleted for secreted acidic cysteine-rich glycoprotein (SPARC), a matricellular glyco-

protein implicated in the synthesis of ECM components (13). A mirror phenotype results from gene invalidation of the collagenase MT1-matrix metalloproteinase (MT1-MMP), which leads to the formation of a rigid network of collagen fibrils and reduced lipid accumulation in the adipocytes (14). These observations suggest that increased ECM deposition in WAT may contribute to restrain adipocyte expansion in obesity.

In humans, the nature of WAT fibrosis and its clinical relevance are poorly documented and have been addressed mostly by gene expression evaluation. Subcutaneous white adipose tissue (scWAT) collagen VI expression is increased in Asian Indian subjects compared with Caucasians, in relation to their higher level of susceptibility to insulin resistance (12). Pasarica et al. (15) showed that the expression of collagen VI in human WAT is upregulated after 8 weeks of overfeeding, concomitant with increased inflammatory gene expression. These two studies suggest that increased collagen VI deposition could be a hallmark of WAT deregulation in obesity.

Here, we aimed to characterize more precisely fibrotic depots in lean and obese subjects and the pathologic relevance of fibrosis in scWAT and omental white adipose tissue (oWAT). First, we analyzed qualitatively and quantitatively fibrosis in scWAT and oWAT of obese and lean subjects. Second, we characterized cells structurally linked with fibrotic depots. Third, we determined if there is a link between the altered metabolic parameters of obese and fibrosis quantified in WAT depots. And fourth, we examined the consequence of fibrosis accumulation in the outcome of body fat loss in the model of gastric bypass.

RESEARCH DESIGN AND METHODS

A total of 65 obese subjects (BMI: 48.2 ± 0.8 kg/m^2, age 39.9 ± 1.4 years) were recruited in the Nutrition Department at the Pitié-Salpêtrière Hospital (Paris, France). Patients met the criteria for obesity surgery, i.e., BMI ≥40 or ≥35 kg/m^2 with at least one comorbidity (hypertension, type 2 diabetes, dyslipidemia, or obstructive sleep apnea syndrome). The subjects had stable weight (i.e., variations of less than ± 2 kg) for at least 3 months before the surgery. Subjects had no acute or chronic inflammatory or infectious disease, viral infection, cancer, or known alcohol consumption (>20g per day). Clinical and biologic parameters were assessed before the gastric bypass surgery and at 3, 6, and 12 months after surgery (data can be found in supplemental Table 1 in the online appendix available at http://diabetes.diabetesjournals.org/cgi/content/full/db10-0585/DC1). According to the criteria of fasting glycemia over 7 mmol/l or the use of an antidiabetic drug, 21 subjects had type 2 diabetes. Three of these individuals required insulin therapy, 13 subjects were treated with metformin and hypolipidemic drugs (either fibrates or statins), and 5 were not treated. Seven female and 2 male volunteers (BMI: 22.8 ± 0.7 kg/m^2, age 46.0 ± 4.2 years) were recruited as a control group in the same clinical protocol. These subjects had abdominal programmed surgery (inguinal hernia, cholecystectomy, hysterectomy, gastro-esophageal reflux). They had no inflammatory state and accepted the realization of omental and subcutaneous biopsies in the same location as that of obese subjects. The Ethics Committee of the Hôtel-Dieu Hospital approved the clinical investigations. Subjects gave a written informed consent after individual explanation.

Clinical and biological parameters. In obese subjects, body composition was estimated by whole-body fan-beam dual energy X-ray absorptiometry scanning (Hologic Discovery W, software v12.6, 2; Hologic, Bedford, MA) (16). To determine body fat and lean mass repartition, we used specific measures and analyses as described (17). Blood samples were collected after an overnight fast of 12 h. Glycemia was measured enzymatically. Serum insulin concentrations were measured using a commercial IRMA kit (Bi-insuline IRMA CisBio International, France). Serum leptin and adiponectin were determined using a radioimmunoassay kit (Linco Research, St. Louis, MO), according to the manufacturer's recommendations, sensitivity: 0.5 ng/ml and 0.8 ng/ml for leptin and adiponectin respectively. Serum level of interleukin-6 (IL-6) was measured by an ultrasensitive ELISA system (Quantikine US, R&D Systems Europe, U.K., sensitivity <0.04 pg/ml). We measured high-sensitivity C-reactive protein (hsCRP) using an IMMAGE automatic immunoassay system (Beckman-Coulter, Fullerton, CA). The sensitivity was 0.02 mg/dl.

Immunohistochemical analysis of adipose tissue. Omental (oWAT) and subcutaneous (scWAT) biopsies were obtained during gastric or abdominal surgery in each individual. A portion of each WAT biopsy was immediately transferred into liquid nitrogen before RNA analysis. The other part was fixed overnight at 4°C in 4% paraformaldehyde, and processed for standard paraffin embedding. Sections of 5 μm were stained as described below and observed under a Zeiss 20 Axiostar Plus microscope (Zeiss, Germany). Digital images were captured by a camera (triCCD, Sony, France). Adipocyte diameters and macrophage number were measured as described (18). We used cell-specific stains targeted to macrophages (HAM56, Dakocytomation, Trappes, France) and to M1 or M2 macrophage subtypes, respectively, CD40 (R&D Systems, Minneapolis, MN) and CD206 (R&D-Systems, Minneapolis, MN), CD3 (Neomarker Microm, Francheville, France) for T-lymphocytes, tryptase (Dakocytomation, Trappes, France) for mast cells. An antibody binding to the α3 chain of the human collagen VI was used (Abcam, Paris, France). Method specificity tests were performed by omission of primary antibodies and use of preimmune serum.

Quantification and characterization of fibrotic depots. Slides of WAT biopsies were stained with picrosirius red. Fibrosis analysis was performed by histomorphometry using an Alphelys platform (Histolab Software, Plaisir, France) with content color thresholds. The quantification of total fibrosis was expressed as the ratio of fibrous tissue area stained with picrosirius red/total tissue surface, as described by Henegar et al. (8). The same procedure was used for quantification of pericellular fibrosis, expressed as the ratio of the sum of stained areas/the sum of field surfaces measured in 10 random fields at ×10 magnification for each biopsy.

Polarized light microscopic observation of WAT fibrosis. We observed the scWAT and oWAT of lean and obese subjects using polarized light microscopy on sirius red staining sections allowing visualization of collagen fibbers with different colors (19). Type I collagen fibbers are orange to red, whereas the thinner type III collagen fibbers appear yellow to green.

Adipocyte versus stroma vascular fraction gene expression by real-time quantitative PCR. In 12 patients, surgical subcutaneous AT samples from lean and obese subjects were separated into adipocytes and stroma vascular fraction (SVF), as by Clement et al. (20). We evaluated the collagen type *1α1*, *3α1*, and *6α1* gene expression changes by reverse transcription and real-time PCR that were performed as by Clement et al. (21). We used 18S rRNA (rRNA Control TaqMan Assay kit, Applied Biosystems, Foster City, CA) as a normalization control. Primer designs can be provided on request.

Isolation of cells from WAT fibrosis and immunofluorescence analysis. The scWAT and oWAT were digested by 1-h collagenase treatment. The digested material was filtered and the nondigested fibrosis was collect from the gauze tissue. After a wash in PBS, fibrosis pieces were put in erythrocyte lysis buffer for 10 min and digested again in trypsin EDTA buffer for 10 min. The digested material was filtered, centrifuged, and cultured on glass coverslips in appropriate media (DMEM 10% FBS for preadipocytes). A fraction of the cells were differentiated in adipocytes as described by Lacasa et al. (22). Immunofluoresence staining was performed as previously described (10).

Clustering analysis. To assess the relationship between fibrosis and bioclinical parameters, we used a recent implementation of the k-means algorithm dedicated to longitudinal data (23). We chose the number of clusters to be three as other values lead to clusters with less than three trajectories.

Statistical analysis. Values are expressed as mean ± SD. The Gaussian distribution of all parameters was tested. Differences between variables were determined with a nonparametric Wilcoxon test (obese vs. lean subjects); Correlations were examined with parametric Pearson or nonparametric Spearman correlation tests, as indicated. For noncontinuous measures, χ^2 tests were used. Results were considered significant when $P < 0.05$. For adjustment (BMI, age, sex, and diabetic state), we applied a multiple linear regression modeling using least squares means. In that case, continuous variables were log transformed. Mannová was used for time series analysis. Statistical analysis was performed with JMP statistics software (SAS Institute, version 8.0, Cary, NC).

RESULTS

Collagen diversity in fibrous depots. We analyzed fibrosis in WAT depots by picrosirius red staining in paired scWAT and oWAT from lean and obese subjects. We observed a difference in collagen distribution patterns according to WAT depots. In scWAT, bundles of collagens fibers were abundant and organized mainly in thick bands (Fig. 1*A*, left panel), whereas in oWAT, fibrous bands appeared more contained, thinner, and they surrounded lobule-like structures (Fig. 1*A*, right panel).

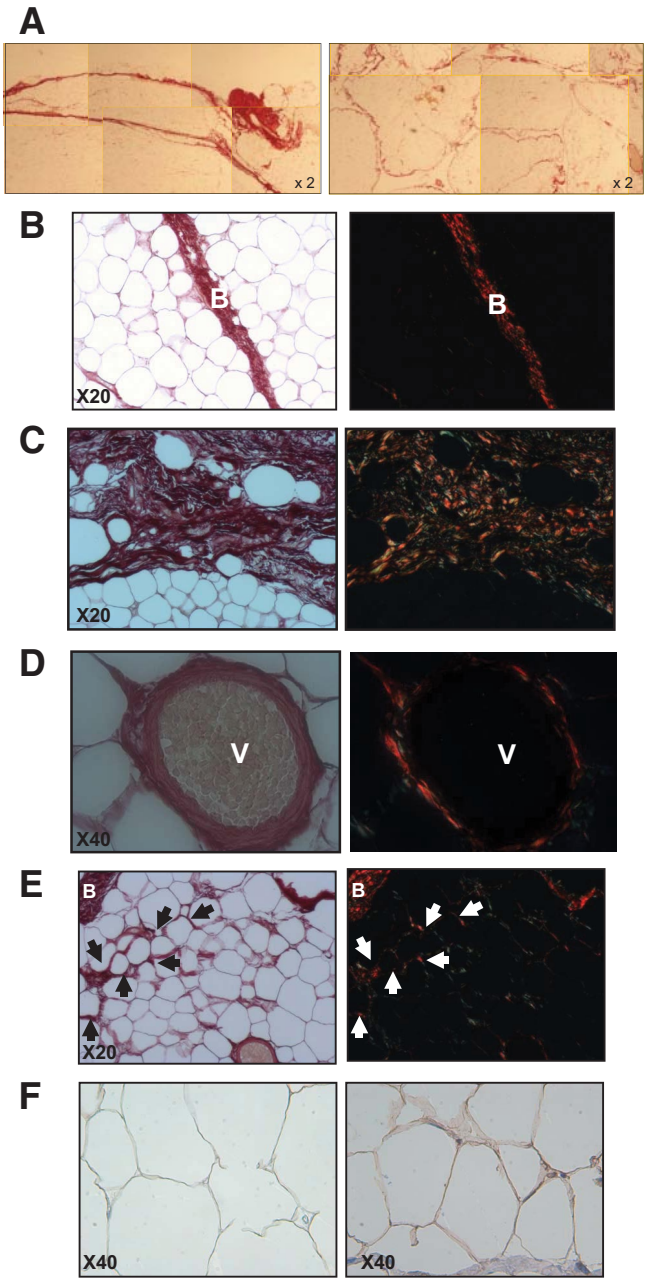

FIG. 1. Picrosirius and collagen VI staining on adipose tissue sections. *A*: Comparison of obese scWAT (*left panel*) and oWAT (*right panel*) sections at low magnification. *B–E*: Omental WAT section with picrosirius staining (*left panels*). Same section observed with polarized light (*right panels*); *arrows* show accumulation of fibrosis around adipocytes (i.e., pericellular fibrosis). *F*: Staining with collagen VI antibody of lean (*left*) and obese oWAT (*right*). V, vessel; B, bundle. (A high-quality digital representation of this figure is available in the online issue.)

Detailed microscopic examination of oWAT slides revealed that collagen fibers are organized in bundles of various thicknesses (Fig. 1*B* and *C*, left panels), containing a few adipocytes isolated from the rest of the parenchyma (Fig. 1*C*). Fibrosis was abundant around vessels (Fig. 1*D*, left panel). Moreover, thinner collagen fibrils surrounded adipocytes localized in areas close to fibrotic bundles, demonstrating pericellular fibrosis (Fig. 1*E*, left panel). Interestingly, these adipocytes were a smaller size (44.4 ± 1.4 μm), compared with fibrosis-free cells located in parenchyma (64.2 ± 2.0 μm, $n = 10$, $P = 0.002$). In lean oWAT sections, this specific collagen deposition around adipocytes was rarely present and found only close to fibrous bundles (data not shown).

When examined with polarized light microscopy, the same slides demonstrated that type I (labeled in red) and type III (labeled in green) collagen fibers were present in bundles of fibrosis (Fig. 1*B–D*, right panels) and around adipocytes (Fig. 1*E*, right panel). Since this technique does not allow visualization of collagen VI, we performed an immunohistochemical staining with an anticollagen VI antibody. Collagen VI deposition was observed around adipocytes (Fig. 1*F*) and in higher amounts in obese (right panel) than in lean oWAT (left panel). In contrast to other collagen isotypes, collagen VI staining was not found within the fibrous bundles.

To substantiate the optic microscopy observations, we explored obese WAT sample with a transmission electron microscopy. Collagen depots were detected between adipocytes (see supplemental Fig. 1). Some collagen fibrils display the characteristic periodic striation suggestive of type I collagen, whereas other collagen fibrils were not organized into fiber structures, a characteristic of type VI collagen.

Abundance of cell types in adipose tissue fibrotic depots. Paired scWAT and oWAT biopsies were stained by hematoxylin/eosine to detect the presence of cells in fibrosis. Although few nuclei were observed in fibrosis bundles in scWAT (Fig. 2*A*, left panel), they were abundantly detected in oWAT fibrosis (Fig. 2*A*, right panel). Thus, fibrosis displays distinct characteristics depending on WAT localization, with more hypocellular fibrosis in scWAT than in oWAT. PCR analysis on paired samples of adipocytes and SVF fractions revealed that expression of three collagens was 4- to 12-fold higher in SVF cells than in adipocytes (Fig. 2*B*), indicating that the main cellular source of collagens in human WAT is within cells of the stromal vascular fraction.

We designed an assay to identify the cells contained in WAT fibrosis (Fig. 2*C*). Since we previously demonstrated that preadipocyte, a fibroblastic-like cell, secretes ECM molecules (10), we characterized the phenotype of the cells released from fibrosis using preadipocytes markers (Fig. 2*D*). Indeed, cells associated with fibrosis were able to differentiate into adipocytes (data not shown) and stained positive for Pref-1, FABP4, and vimentin, three proteins expressed in human preadipocytes (24). Moreover, these cells were also αSMA positive, consistent with a fibroblast-like phenotype and express collagen 1.

Inflammatory cells were identified by immunostaining in fibrous bands in obese oWAT (Fig. 3). Although the presence of CD3+ T-lymphocytes was minimal, we observed abundant amounts of macrophages stained with M1 (CD40) or M2 (CD206) surface markers in the same fibrotic area. Using HAM56 antibody on the same serial slides, we obtained a similar pattern of labeling, indicating that most CD40+ or CD206+ cells were HAM56+ macrophages (data not shown). Additionally, the presence of mast cells and αSMA positive cells were observed in fibrosis bundles at the proximity of the vessels (Fig. 3). A similar pattern of immune cells was identified in scWAT fibrosis (data not shown), although fibrotic bands appeared less enriched in cells in this depot.

Obesity is associated with increased fibrosis in adipose tissue. To evaluate the amount of fibrosis in human WAT, we developed a microscopic image analysis method to quantify pericellular fibrosis surrounding adi-

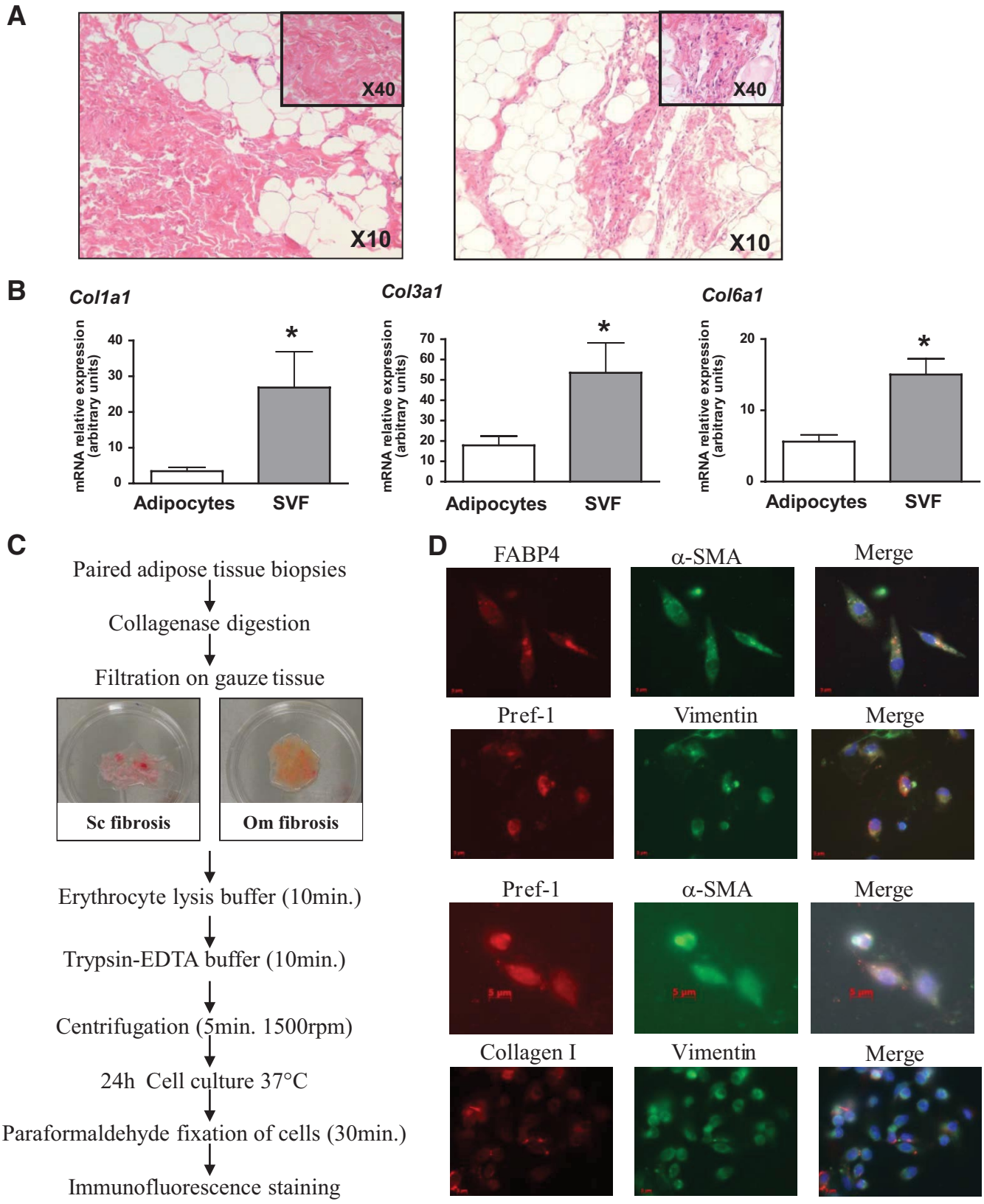

FIG. 2. Cells associated with WAT fibrosis. *A*: Hematoxylin eosine staining on subcutaneous (*left panel*) and omental (*right panel*) WAT sections. *B*: Adipocytes and stroma vascular fraction were isolated from 12 subjects. *COL1A1*, *COL3A1*, and *COL6A1* expression were quantified by real-time PCR. *$P < 0.005$ (*C*) scWAT and oWAT biopsies were digested with collagenase. The nondigested fibrosis was collected. Cells that released from the fibrosis were collected and (*D*) analyzed by immunofluorescence using Pref-1 (red, Cy3-conjugated anti-rabbit IgG), αSMA (green, Cy2-conjugated anti-mouse IgG), FABP4 (red, Cy3-conjugated anti-rabbit IgG), vimentin (green, Cy2-conjugated anti-mouse IgG), and collagen I (red, Cy3-conjugated anti-rabbit IgG). (A high-quality digital representation of this figure is available in the online issue.)

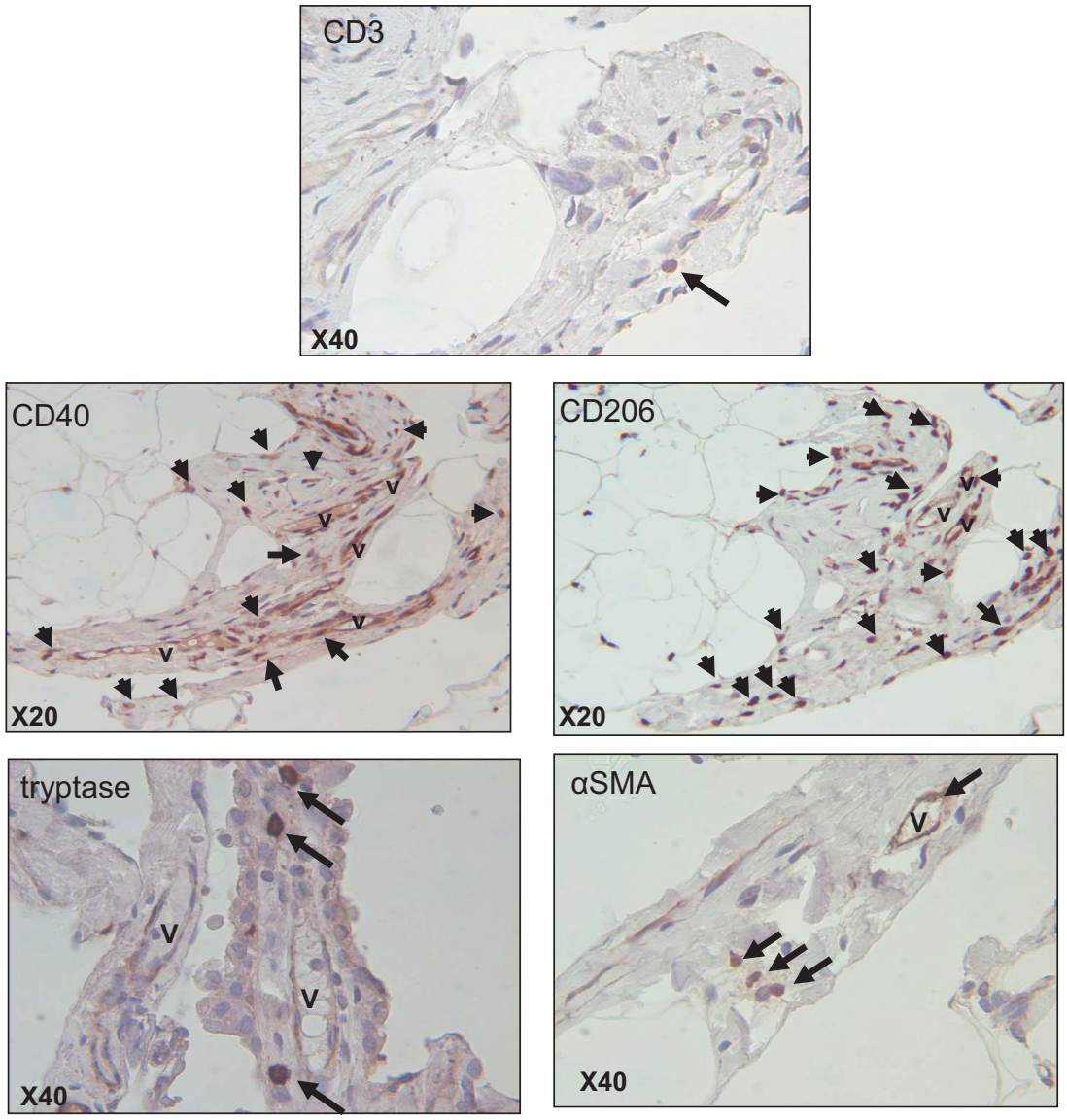

FIG. 3. Identification of different cell types present in obese oWAT fibrosis. Serial sections of human oWAT were stained for markers of T-lymphocytes (CD3), mast cells (tryptase), fibroblastic cells (αSMA), and for CD40+ and CD206+ macrophages. The *arrows* show positive cells in fibrosis area revealed with DAB system (brown staining). Nucleuses were stained with hematoxylin (blue staining). V, vessel. (A high-quality digital representation of this figure is available in the online issue.)

pocytes and total fibrosis, comprising pericellular and fibrosis bundles. The amount of total fibrosis was more than fourfold increased in oWAT of obese versus lean subjects (Fig. 4*A*). No difference was found in scWAT. When pericellular fibrosis was specifically measured, a marked increase was found in obese WAT compared with

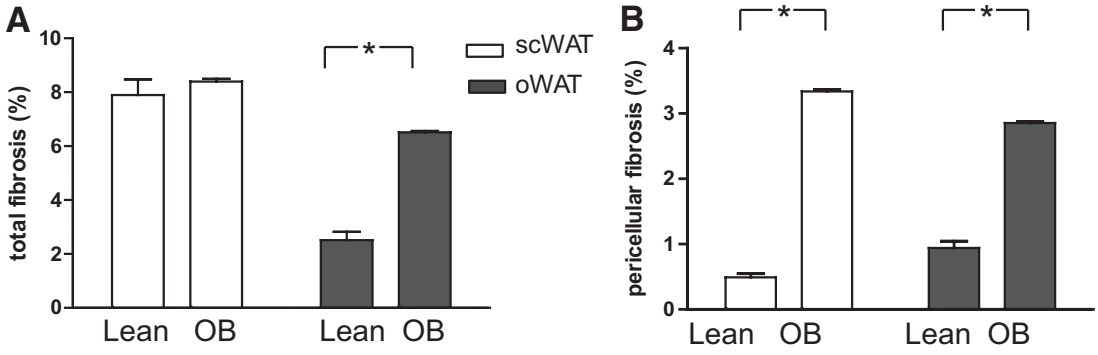

FIG. 4. Total and pericellular fibrosis in WAT of lean and obese subjects. Comparison of total (*A*) and pericellular (*B*) fibrosis in scWAT (*open bars*) and oWAT (*black bars*) of 7 lean and 65 obese (OB) subjects. Data show the amount of fibrotic area as a percentage of the total area as described in RESEARCH DESIGN AND METHODS; *$P < 0.05$.

TABLE 1
Correlation analysis between total fibrosis amount in scWAT and oWAT and clinical characteristics in 65 obese patients

	Fibrosis in scWAT		Fibrosis in oWAT	
	R	*P*	R	*P*
Age	0.06	ns	0.01	ns
Sex*		ns		<0.01
Adiposity markers				
BMI	0.06	ns	0.12	ns
Fat mass	0.11	ns	0.18	ns
Adipocytes diameter	0.01	ns	−0.30	0.02
Plasma parameters				
Triglycerides	0.22	ns	−0.42	<0.01
HDL cholesterol	0.03	ns	0.28	0.03
Apolipoprotein A1	0.05	ns	0.25	0.05
Diabetic status*		ns		ns
Quicki	0.04	ns	0.03	ns
Inflammatory markers				
IL-6	0.20	ns	0.16	ns
hsCRP	0.11	ns	0.07	ns

*Statistical analysis with χ^2 test for noncontinuous measures. ns, not significant; Quicki, quantitative insulin sensitivity check index.

that of lean subjects, whatever the depot (×6.7 in scWAT and ×3 in oWAT in obese vs. lean, Fig. 4*B*). The amounts of both total and pericellular fibrosis in scWAT were positively correlated with the amounts of fibrosis in oWAT measured in the same obese subject ($R = 0.49$ for total fibrosis and $R = 0.34$ for pericellular fibrosis, $P < 0.05$ for both). These data indicate that fibrosis deposition is likely to occur concomitantly in the two adipose tissue sites investigated.

Omental fibrosis associates with adipocyte size and lipid parameters. To examine the pathophysiologic relevance of fibrosis in obese WAT, we investigated the relationships between total fibrosis and clinical and biologic parameters in 65 obese subjects (Table 1). No correlation was found between total fibrosis in oWAT or scWAT and age, BMI, or fat mass in this population. Interestingly, we found that obese men had less fibrosis in oWAT than women. No difference was observed in the amount of fibrosis according to blood-derived glycemic parameters or diabetic status. Circulating IL-6 or hsCRP, two representative markers of systemic inflammation in obesity, did not correlate with fibrosis, whatever the depot. Finally, oWAT, but not scWAT fibrosis, was related to blood lipid parameters, demonstrating a negative correlation with triglycerides and a positive correlation with HDL cholesterol, and Apo lipoprotein A1. Omental fibrosis also negatively correlated with adipocyte size in the same depot.

We performed a multivariate analysis, taking into account sex, diabetic status, and log transformed values of age, BMI, and total omental fibrosis. This analysis confirmed the strong negative association between circulating triglycerides and omental fibrosis. This association remained significant after adding adipocyte diameter in the model, suggesting that these two factors are related to triglyceride levels (supplemental Table 2).

Diminished fat mass loss in gastric bypass associates with subcutaneous adipose tissue fibrosis. The 65 patients were candidate for gastric bypass intervention and were followed for a year with clinical check points at 3, 6, and 12 months after surgery (Table 2). Although gastric bypass is a drastic procedure associated with major body fat loss and reduced adipocyte size, there is a well known individual variation in the amount of weight and fat loss after a year (17). Initial BMI, age, and metabolic state (i.e., diabetes) were shown to be factors modulating the amount of weight loss (25,26). We made the hypothesis that the amount of fibrosis in fat depots associate with fat mass loss. Figure 5*A* shows the decrease of fat mass expressed as a percentage of the initial value.

TABLE 2
Clinical and biologic characteristics of obese subjects before surgery, 3 months, 6 months, and 1 year after surgery

	Before bypass	3 Months after bypass	6 Months after bypass	1 Year after bypass	Mannová (*P* value)
Adiposity markers					
Body weight(kg)	135.03 ± 3.08	111.75 ± 2.84	102.04 ± 2.67	93.39 ± 2.72	< 0.0001
BMI (kg/m^2)	48.21 ± 0.82	39.78 ± 0.78	36.28 ± 0.78	33.30 ± 0.83	< 0.0001
Fat mass (% weight)	46.21 ± 0.69	43.15 ± 0.71	39.24 ± 0.84	34.53 ± 0.89	< 0.0001
Leptin (ng/ml)	63.05 ± 3.16	32.85 ± 2.15	23.9 ± 1.74	18.53 ± 0.89	< 0.0001
Plasma glucose homeostasis					
Glycaemia (mmol/l)	6.55 ± 0.37	5.18 ± 0.13	4.87 ± 0.14	4.74 ± 0.11	< 0.0001
Insulinemia (mU/ml)	19.02 ± 1.81	8.7 ± 0.47	6.9 ± 4.36	7.23 ± 0.99	< 0.0001
Adiponectin (μg/ml)	6.08 ± 0.36	7.77 ± 0.43	9.95 ± 0.83	10.26 ± 0.67	< 0.0001
Diabetic (%)*	32.3	14.3	9.5	8.6	< 0.005
Plasma lipid homeostasis					
Total cholesterol (mmol/l)	5.00 ± 0.12	4.47 ± 0.11	4.36 ± 0.11	4.28 ± 0.10	< 0.0001
Total triglycerides (mmol/l)	1.53 ± 0.10	1.22 ± 0.06	1.08 ± 0.06	0.89 ± 0.04	< 0.0001
HDL cholesterol (mmol/l)	1.28 ± 0.05	1.23 ± 0.04	1.35 ± 0.05	1.50 ± 0.04	< 0.0001
Liver test					
AST	24.51 ± 1.49	28.13 ± 1.59	26.33 ± 5.85	21.18 ± 1.03	0.0035
ALT	35.46 ± 3.49	38.31 ± 3.32	25.33 ± 2.59	24.27 ± 4.29	0.0287
GGT	48.90 ± 5.26	29.75 ± 2.90	40.38 ± 17.55	22.66 ± 2.13	< 0.0001
Inflammatory markers					
Plasma hsCRP (mg/l)	0.91 ± 0.08	0.61 ± 0.09	0.39 ± 0.05	0.33 ± 0.11	< 0.0001
Plasma IL-6 (pg/ml)	3.94 ± 0.32	3.46 ± 0.29	3.22 ± 0.39	2.27 ± 0.38	0.62

*Statistical analysis with McNemar χ^2 test for noncontinuous measures. AST, aspartate aminotransferase; ALT, alanine aminotransferase; GGT, γ-glutamyl transferase.

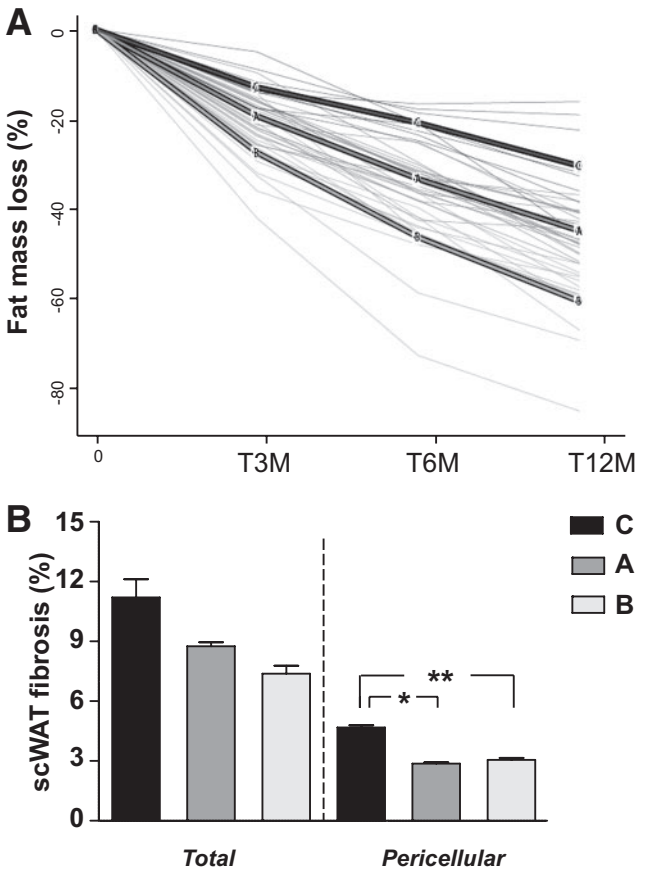

FIG. 5. Clustering of fat mass loss profiles in obese subjects and relation with scWAT fibrosis. *A*: Individual fat mass changes at 3, 6, and 12 months after surgery were clustered using a recently implemented k-means algorithm dedicated to longitudinal data. The panel shows individual fat mass changes expressed as change at 3, 6, or 12 month/time 0 values. Three clusters were built. A, B, and C are the mean of fat-mass changes in each clustered group. *B*: Mean of scWAT total fibrosis or pericellular fibrosis in each clustered group, A, B, and C. Pericellular fibrosis is significantly more abundant in cluster C compared with A and B. *P = 0.01 **P = 0.001.

Using a Spearman correlation test, we found significant negative correlations between the amount of total fibrosis in scWAT before intervention and the percentage of fat mass loss at 3 months (R = −0.39, P = 0.004), 6 months (R = −0.31, P = 0.030), and 12 months (R = −0.30, P = 0.040) after surgery. Similar negative correlations were found between pericellular fibrosis and fat mass loss at 3 months (R = −0.23, P = 0.008), 6 months (R = −0.32, P = 0.020), and 12 months (R = −0.30, P = 0.030).

Since individual responses were highly variable, we used a clustering approach enabling grouping of the subjects in three partitions. Supplemental Table 3 summarizes the clinical differences between the three clustered groups. Subjects in group C lost less body fat mass after surgery compared with A and B groups. Group C subjects had higher BMI, no difference in serum adiponectin, triglycerides, and cholesterol, and markedly increased plasmatic IL-6. This prompted us to perform a multivariate models analysis to explain the percentage of fat mass loss at 3, 6, and 12 months after surgery, using IL-6 and scWAT fibrosis as explicative variables. Adjustment with IL-6 only marginally modified the significant associations between scWAT fibrosis and the percentage of fat mass loss at the follow-up time points (supplemental Table 4).

We then compared fibrotic depots and clinical data before the intervention in the three clustered groups A, B, and C. Subjects in group C demonstrated a trend in increased total fibrosis and significantly higher pericellular fibrosis amount in scWAT (P = 0.008), compared with A or B subject groups (Fig. 5*B*).

DISCUSSION

We performed here a detailed analysis of the nature of fibrosis in two distinct WAT depots and explored its association with clinical parameters of obese patients. We show, for the first time, the presence of different patterns of fibrous depots and detailed collagen fibers organization in human WAT. Fibrosis appears distributed in bundles of variable thickness, which may contain some adipocytes isolated from the rest of the parenchyma. The detailed observation of fibrous structure also shows fibrosis spanning around each adipocyte (i.e., pericellular fibrosis), a fiber disposition that may directly affect adipose cell biology. Interestingly, we observed that some adipocytes engulfed in fibrosis stained negative for perilipin (supplemental Fig. 2), reminiscent of perilipin-negative adipocytes previously described in crown-like structures of macrophages (27). This suggests that fibrosis could be a response to signals emerging from dysfunctional or dying adipocytes.

Type I and III collagens were more frequently observed in fibrous bundles, whereas type VI collagen surrounded parenchymal adipocytes, particularly in obese subjects. Thus, collagen VI may represent a small proportion of total collagens in human WAT, at variance with mouse WAT in which collagen VI is abundantly expressed (11). In a large population of normal weight and overweight males, Pasarica et al. (15) showed that type VI collagen gene expression in scWAT increases with BMI. In our population of subjects with extreme BMI, although we cannot exclude increased collagen VI expression in WAT, no relationship was established between BMI and total collagen quantification based on picrosirius staining.

One important finding of this study is the negative relationship between the amount of oWAT fibrosis and adipocyte size, on the one hand, and circulating triglycerides, on the other hand. Multivariate analysis showed that these factors are closely related, suggesting that omental fibrosis influences the circulating triglycerides level by limiting adipocyte size. The fact that obese patients with smaller adipocyte cell size have a better lipid profile is in agreement with recent observations by Arner E. et al. (2) showing that women with adipocyte hypertrophy have a more adverse metabolic profile than women with cellular hyperplasia at a similar BMI level. Our observation suggests that the generation of omental fibrosis could contribute to limit adipocyte expansion, thus acting as an adaptation mechanism that contributes to slowing down the negative effect of adipocyte hypertrophy. Of note, these relationships were not found in scWAT, suggesting differential consequences of the presence of fibrosis depending on fat depot localization. Additionally, our data suggest that the presence of high levels of fibrosis in WAT does not markedly influence glucose homeostasis, since no significant correlation was found between the amount of fibrosis and glycemic parameters in our population of morbidly obese subjects.

The mechanisms and kinetic of fibrotic depot accumulations are unknown and difficult to study in humans. In particular, the suggested link between fibrotic depots and

immune cells accumulation in obese WAT parenchyma (12,28) does not appear straightforward based on our data. Fibrosis was more abundant in subcutaneous than in omental depots where inflammatory cell accumulation is greater. We found no correlations between fibrosis quantification and systemic low grade inflammation based on IL-6 or C-reactive protein circulating measures. Macrophages of both M1 and M2 phenotype and mast cells were the main immune cells found in fibrotic area, where T lymphocytes were less frequent. Fibrosis is typically considered a fibroproliferative disorder, with the uncontrolled production of ECM components by fibroblasts activated by an inflammatory microenvironment. Although we found αSMA-positive cells in fibrotic bands, immunofluorescence also highlighted that these cells display features of preadipocytes. This is in agreement with our previous experiments in which we showed a capacity of human preadipocytes to secrete fibrotic factors under inflammatory conditions (8,10).

Recent studies suggest that adiponectin exerts antifibrotic effects partly by reducing profibrotic TGF-β signaling in experimental models of liver or cardiac fibrosis (29,30). Although measures were not available for the lean group in this study, it is well established that adiponectin levels are reduced in obesity. This feature could contribute to promotion of fibrosis deposition in WAT. However, our data failed to demonstrate a relationship between adiponectin and WAT fibrosis in the obese group, and lower adiponectinemia did not discriminate subjects included in cluster C characterized by higher amounts of pericellular fibrosis in scWAT (supplemental Table 3). Further studies investigating the evolution of WAT fibrosis in relation with the increase in plasma adiponectin induced by weight loss would help to substantiate the implication of adiponectin in human WAT fibrosis.

Interestingly, we found a negative correlation between the percentage of total fibrosis in scWAT and the percentage of fat mass loss in patients after gastric bypass surgery, a situation leading to drastic fat mass loss and adipocyte shrinkage. Subjects with more WAT fibrosis lose less fat mass at 3, 6, and 12 months after surgery. Although this surgical model is extremely efficient for rapid fat mass loss in obese patients, there is important individual variability in the response to the intervention (31). This is also illustrated by the clustering of individual's fat mass loss after surgery. Classically, subjects with higher BMI before surgery lose more weight and fat mass after bariatric surgery (32). Age and metabolic situation also explain the different weight loss profiles (25). Strikingly, in our study, although group C had higher BMI, they had the less favorable fat loss profile. This group also displayed high levels of IL-6. Of note, the relationship between scWAT fibrosis and resistance to fat mass loss was only slightly influenced after adjustment for IL-6. We suggest that both high levels of scWAT fibrosis and systemic inflammation influenced the individual capacity to lose fat mass in group C subjects. Whether subcutaneous fibrosis could be used as a good predictor of weight loss in surgical or dietary intervention studies, we obviously need more investigations in larger groups of individuals and in those with other nutritional challenges. More studies are also needed to follow the evolution of fibrotic depots after weight loss.

This study provides new insight about the composition in WAT fibrosis showing a different pattern and distinct physiopathologic significance in subcutaneous and omental WAT. Indeed, these two types of fibrosis show differences in their organization, quantity, nature and their influence in the clinical parameters of obese patients. A major finding is the diminished fat mass loss in patients with high level of fibrosis in their subcutaneous adipose tissue, which designs this alteration as a potential predictive factor for resistance to weight loss in obese subjects.

ACKNOWLEDGMENTS

This program was supported by the Commission of European Communities (Collaborative Project ADAPT, contract number HEALTH-F2-2008-201100), Hepadip consortium (http://www.hepadip.org/, contract LSHM-CT-2005-018734), by INSERM. This clinical work was supported by the Programme Hospitalier de Recherche Clinique, Assistance Publique-Hôpitaux de Paris (AOR 02076), the Contrat de Recherche Clinique (to C.P.), and support from Fondation pour la Recherche Medicale (to A.D.).

No potential conflicts of interest relevant to this article were reported.

A.D. performed fibrosis quantification, polarized light microscopic observation, immunohistology and immunofluorescence staining, gene expression experiments, participated in all data analyses and manuscript writing. J.T. performed pericellular fibrosis quantification and electron microscopy, participated in all data analyses and manuscript writing. D.L. helped with experiment design and in vitro experiments, and assisted with data interpretation and manuscript writing. N.V. collected obese tissue samples. D.H. prepared adipose tissue slides for immunohistochemistry. A.A. collected lean tissue samples. A.B., M.G.-M., and P.B. assisted with data interpretation and manuscript writing. C.P. collected all clinical parameters and assisted with manuscript writing. J.-D.Z. performed clustering analysis. K.C. designed the experiments, participated in all data analyses, and prepared the manuscript.

The authors wish to thank Nathalie Colnot, Pathology Department of Beaujon Hospital, and Jean-François Bedel, Centre de Recherche en Nutrition Humaine-Ile de France (Direction de la Recherche Clinique) for picrosirius red staining and fibrosis quantification, and Patricia Bonjour, Anatomopathology Department of Hôtel-Dieu Hospital, for histologic help and support. The authors thank Dr. Florence Marchelli and Mme Christine Baudoin, Centre de Recherche en Nutrition Humaine Ile de France, Pitié-Salpêtrière Hospital, who contributed to clinical and biological data collections in patients and database constitution. Patricia Ancel, Nutrition Department, Pitié-Salpêtrière Hospital, performed the evaluation of adipocyte size. The authors also thank Dr. Valérie Paradis, Pathology Department of Beaujon Hospital, for scientific discussion.

REFERENCES

1. Hotamisligil GS. Inflammation and endoplasmic reticulum stress in obesity and diabetes. Int J Obes (Lond) 2008;32 Suppl 7:S52–S54
2. Arner E, Westermark PO, Spalding KL, Britton T, Ryden M, Frisen J, Bernard S, Arner P. Adipocyte turnover: relevance to human adipose tissue morphology. Diabetes 2010;59:105–109
3. Skurk T, Alberti-Huber C, Herder C, Hauner H. Relationship between adipocyte size and adipokine expression and secretion. J Clin Endocrinol Metab 2007;92:1023–1033
4. Spiegelman BM, Ginty CA. Fibronectin modulation of cell shape and lipogenic gene expression in 3T3-adipocytes. Cell 1983;35:657–666
5. Pierleoni C, Verdenelli F, Castellucci M, Cinti S. Fibronectins and basal

lamina molecules expression in human subcutaneous white adipose tissue. Eur J Histochem 1998;42:183–188
6. Lijnen HR. Angiogenesis and obesity. Cardiovasc Res 2008;78:286–293
7. Wynn TA. Common and unique mechanisms regulate fibrosis in various fibroproliferative diseases. J Clin Invest 2007;117:524–529
8. Henegar C, Tordjman J, Achard V, Lacasa D, Cremer I, Guerre-Millo M, Poitou C, Basdevant A, Stich V, Viguerie N, Langin D, Bedossa P, Zucker JD, Clement K. Adipose tissue transcriptomic signature highlights the pathologic relevance of extracellular matrix in human obesity. Genome Biol 2008;9:R14
9. Mutch DM, Tordjman J, Pelloux V, Hanczar B, Henegar C, Poitou C, Veyrie N, Zucker JD, Clement K. Needle and surgical biopsy techniques differentially affect adipose tissue gene expression profiles. Am J Clin Nutr 2009;89:51–57
10. Keophiphath M, Achard V, Henegar C, Rouault C, Clement K, Lacasa D. Macrophage-secreted factors promote a profibrotic phenotype in human preadipocytes. Mol Endocrinol 2009;23:11–24
11. Liu J, Divoux A, Sun J, Zhang J, Clement K, Glickman JN, Sukhova GK, Wolters PJ, Du J, Gorgun CZ, Doria A, Libby P, Blumberg RS, Kahn BB, Hotamisligil GS, Shi GP. Genetic deficiency and pharmacological stabilization of mast cells reduce diet-induced obesity and diabetes in mice. Nat Med 2009;15:940–945
12. Khan T, Muise ES, Iyengar P, Wang ZV, Chandalia M, Abate N, Zhang BB, Bonaldo P, Chua S, Scherer PE. Metabolic dysregulation and adipose tissue fibrosis: role of collagen VI. Mol Cell Biol 2009;29:1575–1591
13. Bradshaw AD, Graves DC, Motamed K, Sage EH. SPARC-null mice exhibit increased adiposity without significant differences in overall body weight. Proc Natl Acad Sci U S A 2003;100:6045–6050
14. Chun TH, Hotary KB, Sabeh F, Saltiel AR, Allen ED, Weiss SJ. A pericellular collagenase directs the 3-dimensional development of white adipose tissue. Cell 2006;125:577–591
15. Pasarica M, Gowronska-Kozak B, Burk D, Remedios I, Hymel D, Gimble J, Ravussin E, Bray GA, Smith SR. Adipose tissue collagen VI in obesity. J Clin Endocrinol Metab 2009;94:5155–5162
16. Perlemuter G, Naveau S, Belle-Croix F, Buffet C, Agostini H, Laromiguiere M, Cassard-Doulcier AM, Oppert JM. Independent and opposite associations of trunk fat and leg fat with liver enzyme levels. Liver Int 2008;28:1381–1388
17. Ciangura C, Bouillot JL, Lloret-Linares C, Poitou C, Veyrie N, Basdevant A, Oppert JM. Dynamics of change in total and regional body composition after gastric bypass in obese patients. Obesity (Silver Spring), 2009
18. Cancello R, Tordjman J, Poitou C, Guilhem G, Bouillot JL, Hugol D, Coussieu C, Basdevant A, Bar Hen A, Bedossa P, Guerre-Millo M, Clement K. Increased infiltration of macrophages in omental adipose tissue is associated with marked hepatic lesions in morbid human obesity. Diabetes 2006;55:1554–1561
19. Sund S, Grimm P, Reisaeter AV, Hovig T. Computerized image analysis vs semiquantitative scoring in evaluation of kidney allograft fibrosis and prognosis. Nephrol Dial Transplant 2004;19:2838–2845
20. Clement K, Viguerie N, Poitou C, Carette C, Pelloux V, Curat CA, Sicard A, Rome S, Benis A, Zucker JD, Vidal H, Laville M, Barsh GS, Basdevant A, Stich V, Cancello R, Langin D. Weight loss regulates inflammation-related genes in white adipose tissue of obese subjects. FASEB J 2004;18:1657–1669
21. Clement K, Viguerie N, Diehn M, Alizadeh A, Barbe P, Thalamas C, Storey JD, Brown PO, Barsh GS, Langin D. In vivo regulation of human skeletal muscle gene expression by thyroid hormone. Genome Res 2002;12:281–291
22. Lacasa D, Taleb S, Keophiphath M, Miranville A, Clement K. Macrophage-secreted factors impair human adipogenesis: involvement of proinflammatory state in preadipocytes. Endocrinology 2007;148:868–877
23. Genolini C, Falissard B: Kml: k-means for longitudinal data. Computational Stat, 2009;25:317–328
24. Rathod MA, Rogers PM, Vangipuram SD, McAllister EJ, Dhurandhar NV. Adipogenic cascade can be induced without adipogenic media by a human adenovirus. Obesity (Silver Spring) 2009;17:657–664
25. Campos GM, Rabl C, Mulligan K, Posselt A, Rogers SJ, Westphalen AC, Lin F, Vittinghoff E. Factors associated with weight loss after gastric bypass. Arch Surg 2008;143:877–883; discussion 884
26. Perugini RA, Mason R, Czerniach DR, Novitsky YW, Baker S, Litwin DE, Kelly JJ. Predictors of complication and suboptimal weight loss after laparoscopic Roux-en-Y gastric bypass: a series of 188 patients. Arch Surg 2003;138:541–545; discussion 545–546
27. Cinti S, Mitchell G, Barbatelli G, Murano I, Ceresi E, Faloia E, Wang S, Fortier M, Greenberg AS, Obin MS. Adipocyte death defines macrophage localization and function in adipose tissue of obese mice and humans. J Lipid Res 2005;46:2347–2355
28. Strissel KJ, Stancheva Z, Miyoshi H, Perfield JW 2nd, DeFuria J, Jick Z, Greenberg AS, Obin MS. Adipocyte death, adipose tissue remodeling, and obesity complications. Diabetes 2007;56:2910–2918
29. Kamada Y, Tamura S, Kiso S, Matsumoto H, Saji Y, Yoshida Y, Fukui K, Maeda N, Nishizawa H, Nagaretani H, Okamoto Y, Kihara S, Miyagawa J, Shinomura Y, Funahashi T, Matsuzawa Y. Enhanced carbon tetrachloride-induced liver fibrosis in mice lacking adiponectin. Gastroenterology 2003;125:1796–1807
30. Fujita K, Maeda N, Sonoda M, Ohashi K, Hibuse T, Nishizawa H, Nishida M, Hiuge A, Kurata A, Kihara S, Shimomura I, Funahashi T. Adiponectin protects against angiotensin II-induced cardiac fibrosis through activation of PPAR-α. Arterioscler Thromb Vasc Biol 2008;28:863–870
31. Buchwald H, Avidor Y, Braunwald E, Jensen MD, Pories W, Fahrbach K, Schoelles K. Bariatric surgery: a systematic review and meta-analysis. JAMA 2004;292:1724–1737
32. Flancbaum L, Choban PS, Bradley LR, Burge JC. Changes in measured resting energy expenditure after Roux-en-Y gastric bypass for clinically severe obesity. Surgery 1997;122:943–949